Reaching out for signals: filopodia sense EGF and respond by directed retrograde transport of activated receptors

Diane S. Lidke, Keith A. Lidke, Bernd Rieger, Thomas M. Jovin, and Donna J. Arndt-Jovin

Department of Molecular Biology, Max Planck Institute for Biophysical Chemistry, 37077 Goettingen, Germany

ErbB1 receptors situated on cellular filopodia undergo systematic retrograde transport after binding of the epidermal growth factor (EGF) and activation of the receptor tyrosine kinase. Specific inhibitors of the erbB1 receptor tyrosine kinase as well as cytochalasin D, a disruptor of the actin cytoskeleton, abolish transport but not free diffusion of the receptor–ligand complex. Diffusion constants and transport rates were determined with single molecule sensitivity by tracking receptors labeled with EGF conjugated to fluorescent quantum dots. Retrograde transport precedes receptor endocytosis, which occurs at the base of the filopodia. Initiation of transport requires the interaction and concerted activation of at least two liganded receptors and proceeds at a constant rate mediated by association with actin. These findings suggest a mechanism by which filopodia detect the presence and concentration of effector molecules far from the cell body and mediate cellular responses via directed transport of activated receptors.

Introduction

ErbB1 (EGFR, HER2), the prototype of Class I transmembrane receptor tyrosine kinases, is the receptor for epidermal growth factor (Jorissen et al., 2003). Activation induced by the extracellular binding of EGF triggers several signaling cascades responsible for cellular motility, DNA replication, and cell division. Despite the recent crystallographic elucidation of the complex of the erbB1 ectodomain with EGF (Garrett et al., 2002; Ogiso et al., 2002) and intensive cellular and biochemical investigations of the receptor over the past 20 yr, fundamental questions remain concerning the structural determinants of receptor affinity, association states, internalization dynamics, and intracellular trafficking and signaling (Yarden and Sliwkowski, 2001; Schlessinger, 2002; Mattoon et al., 2004). These issues are of biomedical importance given that the overexpression and mutation of erbB1 and the three other members of the erbB family are linked to many types of cancer (for review see Marmor et al., 2004).

We recently demonstrated that complexes of streptavidin-conjugated quantum dots (QDs) with biotinylated EGF (EGF-QD) are biochemically competent ligands for erbB1 and that their unique fluorescence properties (brightness, selectivity, and photostability) meet the requirements for prolonged in vivo imaging (Lidke et al., 2004). We detected a previously unreported retrograde transport of activated erbB1 receptors on cellular filopodia and postulated that it might be linked directly or indirectly to the cytoskeleton.

The cytoskeleton is composed of dynamic networks of polymerized actin and tubulin and numerous associated proteins that facilitate the trafficking of proteins and organelles involved in cell motility, endocytosis, and signaling. Filopodia are elongated, thin cellular processes with a core of actin bundles (Small et al., 2002). Their constituent actin filaments have pointed ends oriented toward the interior of the cell and undergo growth and exchange by the concerted addition of monomers to the distal plus ends and depolymerization from the minus ends, a process denoted as treadmilling. Concurrently, F-actin is actively transported toward the cell interior by motor proteins (Mallavarapu and Mitchison, 1999). These processes result in a net retrograde flow of F-actin. Passive association with actin subunits of the filaments results in the retrograde progression of associated macromolecules and their cargo toward the cell body, whereas molecular motors are capable of actively transporting along actin in either direction (Small et al., 2002; Loomis et al., 2003).

In the present study, we examined in detail the binding of ligand to the erbB1 receptor and its subsequent retrograde
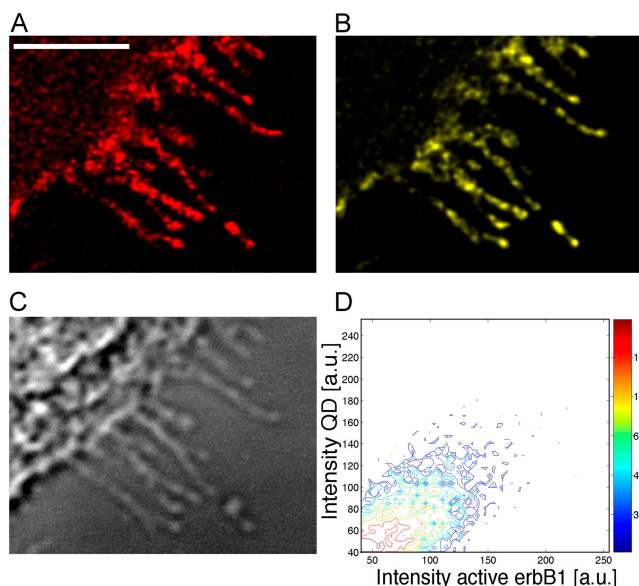
Figure 1. **Activation of erbB1 by binding of EGF-QD.** A431 cells expressing endogenous erbB1 after incubation with 1 nM EGF-QD for 15 min at 4°C followed by 5 min at 37°C were fixed in 4% PFA and immunostained with anti-activated erbB1 and Cy5 GAMIG. (A) QD signal. (B) Activated erbB1. (C) DIC image. (D) Two-dimensional histogram showing the correlation between QD signal and antibody signal. Stacks of three confocal images at each wavelength were deconvolved. Bar, 5 μm.

transport, including the effects of agents that perturb receptor activation and/or the cytoskeleton. We show by quantitative, spectrally resolved, real-time imaging with single molecule (QD) sensitivity that (a) specific inhibitors of the erbB1 kinase as well as cytochalasin D, a disruptor of F-actin, abrogate retrograde transport, whereas the binding of nocodazole, an inhibitor of microtubulin dynamics, has no effect; (b) the initiation of retrograde transport requires the cooperative interaction of at least two activated receptors and proceeds at a constant rate

similar to that of actin flow in the same filopodium; and (c) the ligand–receptor complex is endocytosed only upon reaching the lamellipodial base of the filopodia. We propose that the filopodia serve as sensory organelles probing for the presence and concentration of effector molecules far from the cell body. ErbB1 receptors on the filopodia become activated when ligand exceeds a threshold concentration, triggering transport back to the cellular machinery required for signal transduction.

Results

Binding and activation of EGF-QD on filopodia

Addition of the EGF-QD ligand to epidermal cells led to rapid binding to erbB1 receptors on the cell surface, including filopodia from which they were transported toward the cell body (Lidke et al., 2004). Activation of the receptor occurred on the filopodia during transport as shown in Fig. 1, demonstrating a direct correlation (Fig. 1 D) between the signals from the EGF-QD and those for activated erbB1 (anti-erbB1 phosphotyrosine-1068). The signals were discrete; i.e., activation was restricted to each EGF-QD–erbB1 locus and did not extend to regions between them. The transport of EGF-QD–erbB1 complexes along the filopodia can be viewed in Fig. 2 A and Video 1 (available at http://www.jcb.org/cgi/content/full/jcb.200503140/DC1).

Rate of retrograde transport and the effects of inhibitors

We used quantitative microscopy to distinguish between the processes of random diffusion and directed transport of surface-bound EGF-QDs. Tracks of EGF-QD–erbB1 complexes undergoing retrograde transport on a filopodium showed diagonal trajectories when viewed as x-t and y-t projections (Fig. 2 A, kymograph), indicative of a uniform rate of motion with a

Figure 2. **Quantitative evaluation of receptor diffusion and retrograde transport.** (A) Retrograde transport of EGF-QD–erbB1s on filopodia of living A431 cells expressing endogenous erbB1 and erbB1-eGFP. (top left) Magnified region of the cell periphery showing filopodia (green) with bound EGF-QDs (red). Kymograph of the EGF-QD fluorescence signals on the selected filopodium showing x versus time (bottom left) and y versus time (top right). The QD loci move down the filopodia toward the cell body (located in the bottom left corner of the image), resulting in a net movement left in x and down in y. Loci that do not transport remain in the same place over time and show a vertical (x) and horizontal (y) line in the projections. The turquoise line traces one locus that transported and the green line one that did not. Bar, 5 μm. See also Video 1, available at http://www.jcb.org/cgi/content/full/jcb.200503140/DC1. (B) Typical MSD plots of EGF-QD–erbB1 complexes under different conditions: untreated (blue), nocodazole (red), cytochalasin D (green), and PD153035 (black). (C) Typical trajectory (left) and MSD plot (right) for an EGF-QD–erbB1 loci undergoing diffusion on a cell treated with PD153035. The first 10 points of the MSD plot were fit to MSD = $2D\Delta t$ (red line). (D) Typical trajectory (left) and RMSD plot (right) for an EGF-QD–erbB1 loci undergoing directed transport on an untreated cell. The RMSD plots were fit to RMSD = $v\Delta t$ (red line).
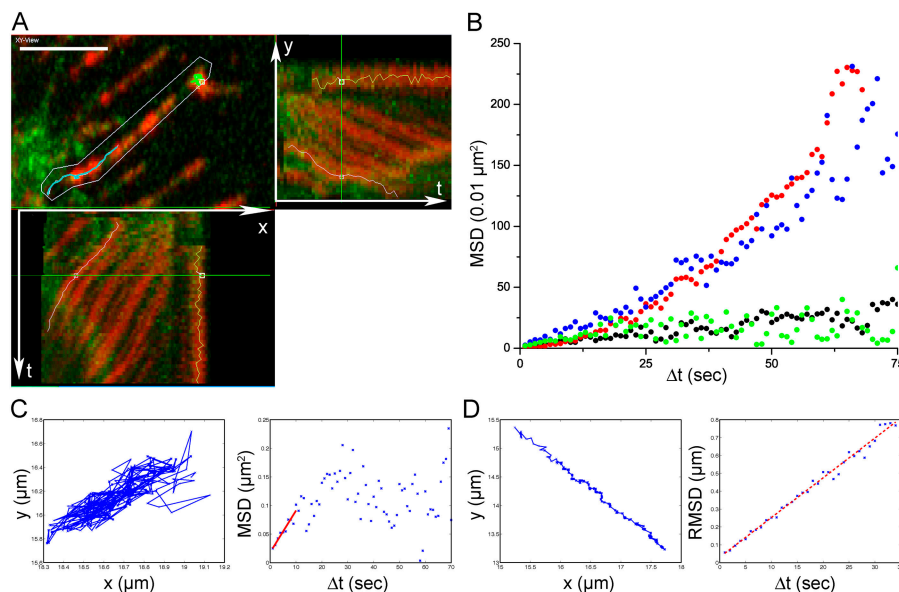
Table I. **Parameters derived from MSD trajectories**

Cell type	Inhibitor	Temp.	$D \times 10^{-11}$	v	n
		°C	cm²/s	nm/s	
A431	-	23		18 ± 10	19
A431-erbB3-mCit	-	23		16 ± 8	7
A431	Cytochalasin D	23	4.2 ± 3		24
A431	Nocodazole	23		10 ± 8	18
A431	PD153035	23	3.8 ± 3		13
A431	-	37		23 ± 20	7
HeLa	-	37		16 ± 2	4
HeLa	-	30		26 ± 14	19
MCF7-erbB1-Δ989–994	-	30		27 ± 19	8

Values reported as weighted mean ± SD. D, diffusion constant; v, velocity; n, number of loci tracked.

directional velocity (in this case) $v = 22 \pm 2$ nm/s (A431 cells, EGF-QD added at room temperature; Fig. 2 A and Video 1).

Retrograde transport was disrupted by PD153035, a specific kinase inhibitor of erbB1 (Fry et al., 1994), and by cytochalasin D (Goddette and Frieden, 1986), an inhibitor of actin polymerization, but not by nocodazole (Jordan et al., 1992), a disruptor of microtubule dynamics (EGF-QD binding and movement in the presence of these inhibitors can be viewed in Videos 2 and 3, available at http://www.jcb.org/cgi/content/full/jcb.200503140/DC1). Typical mean square displacement (MSD) plots of QD loci in the absence or presence of the inhibitors are shown in Fig. 2 (B–D). The movement on cells treated with nocodazole was similar to that on control cells. The corresponding MSDs (Fig. 2 B, red and blue points, respectively) exhibited a behavior characteristic of predominantly vectorial transport (MSD = $v^2\Delta t^2$, where Δt is the time interval).

Exposure of cells to cytochalasin D or PD153035 did not inhibit EGF-QD binding, but the ensuing movement of the complexes displayed a constrained diffusional component as evidenced by a plateau in the MSD versus Δt plots (Fig. 2 B, green and black points, respectively); i.e., retrograde transport was blocked. The size of the restricted diffusion area was found to be 0.15–0.3 μm². In Fig. 2 (C and D), typical traces of EGF-QD–erbB1 complexes undergoing diffusion or directed transport, respectively, can be seen. For estimating the transport velocities, the root MSDs (RMSDs) were used (RMSD = $v\Delta t$; Fig. 2 D). We conclude that at least two conditions must be fulfilled to promote retrograde movement: (a) the erbB1 receptor tyrosine kinase must be activated and (b) the central filopodial actin bundle must remain intact.

Retrograde-directed transport of EGF-activated erbB1 on filopodia was not unique to A431 cells expressing high levels of receptors but also occurred on HeLa cells with only 60,000 endogenous erbB1 receptors or on MCF7 cells transfected with erbB1 (velocity data for these cell types are included in Table I). Transport on these cells was also inhibited by PD153035 and cytochalasin D.

Simultaneous tracking of the activated erbB1 receptor with EGF-QD and measurement of actin flow in filopodia of HeLa cells were performed by photobleaching the expressed eGFP-actin at the loci of transporting QDs (Fig. 3). The displacement of photobleached eGFP-actin segments paralleled that of transporting QDs, suggesting that transport involves coupling to the actin filament.

Table I summarizes the values for transport velocities and diffusion coefficients derived from MSD plots with and without inhibitors and for different cell types and temperatures. At room temperature, similar transport rates of 10–20 nm/s were obtained in untreated cells and cells treated with nocodazole. A significant change in velocity was not observed at higher temperatures. The velocity of retrograde transport was similar in all cell types despite the differences in receptor density, indicating the existence of a conserved mechanism.

The diffusion constants determined from PD153035- and cytochalasin-treated cells for erbB1 of 3–4 × 10^{-11} cm²/s are lower than the values in the literature of 1–5 × 10^{-10} cm²/s determined from FRAP (Zidovetzki et al., 1981; Hillman and Schlessinger, 1982) or single particle tracking (Kusumi et al., 1993). The erbB1 receptors situated on the filopodia do not constitute a unique fraction of receptors in that they exchange freely with molecules on the main cell body, as can be observed in Fig. 4 for data from a FRAP experiment. Diffusion coefficients were determined on the cell body for unliganded ($6 \times 10^{-10} \pm 3 \times 10^{-10}$ cm²/s; $n = 12$) and liganded ($4 \times 10^{-10} \pm 1 \times 10^{-10}$ cm²/s; $n = 11$) erbB1-eGFP expressed in A431 cells from such data. The values for the liganded receptor derived from both the eGFP and fluorescent EGF (Alexa 546) signals were the same.

Transport requires dimerization of erbB1–ligand complexes

In our previous study, we demonstrated that monovalent EGF-QD is capable of binding to and inducing the internalization of erbB1 (Lidke et al., 2004). However, these binding experiments were conducted at ligand concentrations that were not limiting
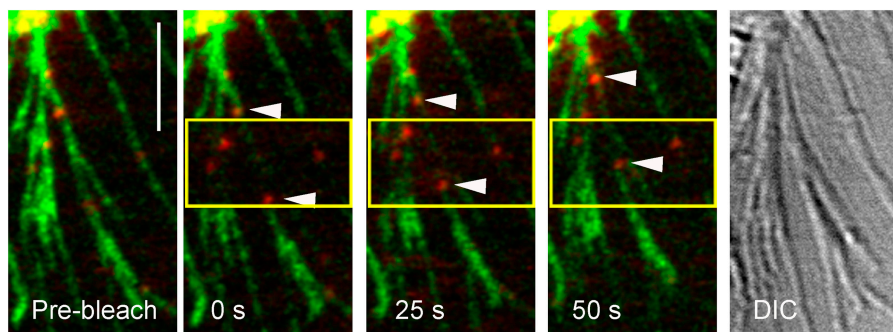
Figure 3. **Simultaneous tracking of GFP-actin and EGF-QD–erbB1.** Selected frames from time series of EGF-QD–erbB1 (red) undergoing transport on the filopodia of HeLa cells expressing GFP-actin (green). After bleaching of GFP-actin (in yellow box), the QDs (arrowheads) are transported to the cell body (top left corner) at the same rate as the unbleached GFP-actin. (right) DIC image of filopodia. Images are single 1-μm confocal sections, Gaussian filtered, and contrast enhanced. Bar, 5 μm.
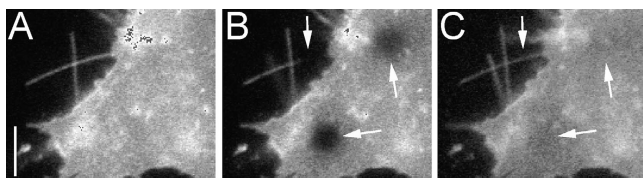
Figure 4. **FRAP of unliganded erbB1-eGFP on filopodia and cell membrane.** (A) Frame before bleaching; (B) first frame after bleaching; (C) frame 10 s into the recovery curve. Arrows indicate the photobleached regions. Bar, 5 μm.

(2 nM). Due to the brightness and photostability of QDs, single molecules can be tracked for extended periods of time (Dahan et al., 2003). Direct proof that a single complex of EGF-QD with erbB1 is not transport competent was obtained by carrying out binding at very low concentrations of EGF-QD (5 pM for a short time), such that only one isolated EGF-QD–erbB1 complex formed on a filopodium. These EGF-QD loci exhibited only diffusive behavior. At 5 min, 100 pM of unlabeled EGF was added, resulting in the rapid initiation of the transport of the EGF-QD–erbB1 complex toward the cell body (Fig. 5, A and B). The inability of isolated (monomeric), ligand-bound, but presumably nonactivated, receptors to engage in retrograde transport is an important new finding of this study.

We often observed the merging of two EGF-QD loci and a concomitant increase in fluorescence intensity when EGF-QD motion changed from diffusion to directed transport (Fig. 5, C and D; and Video 4, available at http://www.jcb.org/cgi/content/full/jcb.200503140/DC1). This result implied a requirement for dimerization or higher order oligomerization of activated erbB1 before the onset of transport, which characteristically commenced following a short lag (∼10 s) after the increase in intensity. That dimerization was sufficient was corroborated by an alternative approach in which we mixed two different colors of EGF-QD ligands at low concentrations and acquired a time series of images using a charge coupled device camera with which single QDs of both types were readily detectable. After merging of the two colors and a lag time of a few seconds, diffusion of the individual particles changed to transport of the joint nanoparticles (Fig. 5, E and F; and Video 5, available at http://www.jcb.org/cgi/content/full/jcb.200503140/DC1). These data and the inhibition of retrograde transport by erbB1-specific kinase inhibitors (Fig. 2, B and C; and Video 2) demonstrate that the minimum requirement for activation and subsequent transport is the formation of a 2:2 EGF–erbB1 dimer complex, consistent with the hypothesis that activation of erbB1 requires the binding of two ligands to a receptor homodimer (Lemmon et al., 1997; Schlessinger, 2002). However, at the EGF-QD concentrations between 100 and 200 pM used in most experiments, we observed a distribution of signal intensities compatible with the transport as a cohort of either closely packed dimers or higher order oligomers. The latter were demonstrated in previous studies based on rotational diffusion measurements with triplet probes (Zidovetzki et al., 1981).

Although EGF-QDs bound to receptors in the presence of the erbB1 kinase inhibitor, the affinity for the ligand was reduced, as evidenced by the loss of bound QDs upon dilution.
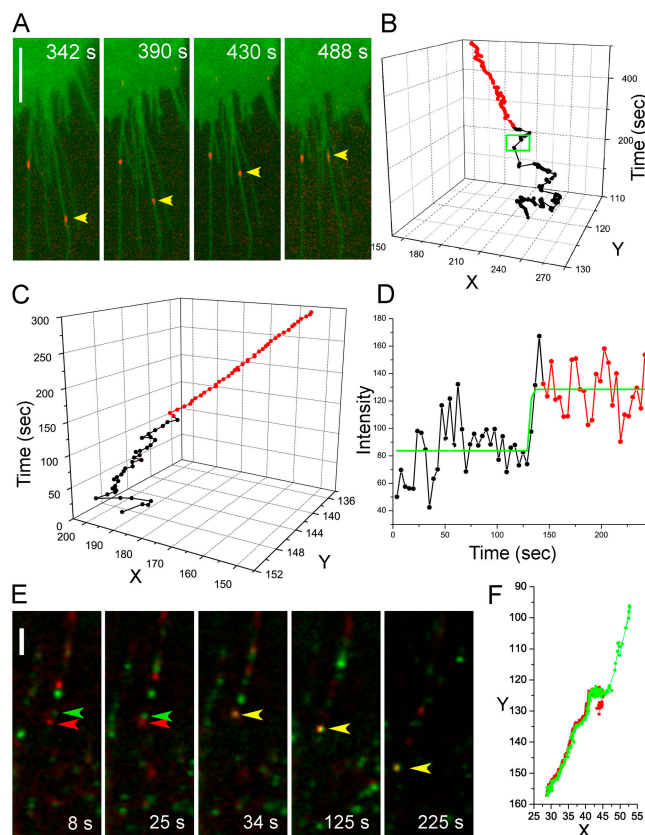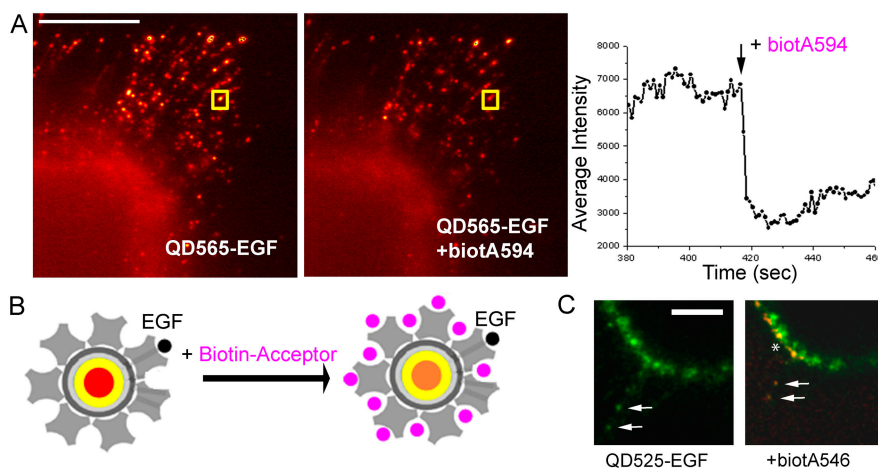

Figure 5. **Oligomerization is required for retrograde transport.** (A) Selected frames of an A431-erbB1-eGFP cell (green) from a time series after binding 5 pM EGF-QD (red) followed by addition of free EGF (50 ng/ml) at 300 s. Bar, 5 μm. Images are contrast enhanced. (B) Trajectory of the indicated monomer EGF-QD–erbB1 complex (A, arrowhead) on a filopodium that exhibits random diffusional movement (black) until the addition of unlabeled EGF (green box), after which the complex commences active retrograde transport (red). (C) Trajectory of EGF-QD–erbB1 complex on a filopodium of an A431 cell. The locus initially undergoes diffusion (black) before active transport begins (red). (D) Plot of intensity versus time of the locus in the trajectory in C. See also Video 4, available at http://www.jcb.org/cgi/content/full/jcb.200503140/DC1. (E) Time series of two different colored EGF-QD–erbB1 complexes (EGF-QD525 tracked by green arrowhead and EGF-QD605 tracked by red arrowhead) on a single filopodium of an A431 cell showing merging (yellow arrowhead) followed by transport to the cell body (bottom left). See also Video 5, available at http://www.jcb.org/cgi/content/full/jcb.200503140/DC1. Bar, 5 μm. Images are contrast enhanced. (F) Trajectory of the two loci in D before and after dimerization.

This observation is compatible with the increased dissociation rates reported by Mattoon et al. (2004) for EGF bound to cells expressing mutant receptors that are dimerization incompetent and fail to autophosphorylate.

Filopodial retrograde transport of erbB1 occurs before endocytosis

To determine whether the receptor complexes were internalized (endocytosed) before, during, or after retrograde transport, we examined the accessibility of the EGF-QD–erbB1 complex on A431 cells to the external medium using two strategies. The first was based on the known reversibility of receptor-bound EGF upon exposure to acidic conditions (Haigler et al., 1980). Washing with 10 mM HCl in 150 mM NaCl caused immediate

Figure 6. **EGF-QD–erbB1s undergo retrograde transport before endocytosis.** (A) Two images selected from a time series just before (left) and after (right) addition of biocytin-Alexa 594 (biotA594) to EGF-QDs undergoing retrograde transport on the filopodia of A431 cells. (right) Relative fluorescence intensity over time of the EGF-QD in the yellow box undergoing transport, demonstrating strong quenching. Bar, 10 μm. (B) Cartoon depicting the experiment: at the loading ratio of EGF/QD used, there are still free sites on the streptavidin conjugate layer available for biotin-acceptor (pink), the binding of which results in FRET-induced quenching of the QD donor fluorescence and concomitant sensitized emission of the acceptor fluorescence. (C) Sensitized emission localizes the sites of internalization to the base of the filopodia. (left) EGF-QD525–erbB1 complexes (green) in the cell membrane being transported on the filopodia (arrows). (right) Upon addition of biotA546, the QD signal is quenched and the sensitized emission of the acceptor (red) can be seen on the filopodial loci and the cell surface (*), whereas the complexes already internalized remain green. Images are maximum intensity projections of two 1.0-μm optical sections, Gaussian filtered, and contrast enhanced. Bar, 10 μm.

release of the QDs from the filopodia (Fig. S2, available at http://www.jcb.org/cgi/content/full/jcb.200503140/DC1). The second technique avoided the adverse condition of extreme pH by exploiting the property of QDs as donors for fluorescence resonance energy transfer (FRET; Clapp et al., 2004; Grecco et al., 2004). At the EGF/QD loading ratios used in our experiments, the QDs retained free biotin binding sites. Thus, the addition of a membrane-impermeable, biotinylated fluorophore with an absorption peak corresponding to the QD emission band should result in quenching by FRET only of QDs accessible to the extracellular buffer; i.e., not yet internalized (Fig. 6 B). In these studies, two combinations of donor-acceptor pairs were used: EGF-QD525 with biocytin-Alexa546 and EGF-QD565 with biocytin-Alexa594. In both cases, addition of the potential acceptor to the medium led to an immediate (within 1 s) and substantial (50–60%) quenching of QDs bound to or transporting on the filopodia (Fig. 6 A). The amount of quenching observed was consistent with control experiments in which the acceptor was added to QDs fixed to a coverslip or in a cuvette. In contrast, QDs already internalized at the base of the filopodia or located elsewhere within the cell were unaffected. The FRET effect was confirmed by observing emission of the Alexa546 bound to the external EGF-QD525–erbB1 as seen in Fig. 6 C in which the QDs on the filopodium (arrows) and the cell surface (asterisk) are seen in yellow and internalized QDs in green.

We determined that clathrin, a component of the clathrin-coated pits presumed to be the entry sites for endocytosis, is restricted to the cell body by immunostaining (Fig. S2). This result was consistent with earlier studies of Semliki Forest Virus uptake (Helenius et al., 1980) in which clathrin was shown to be absent on filopodia and microvilli but clustered at the base of these structures (Hasson and Mooseker, 1995; Small et al., 2002), the site of viral entry.

Is the interaction of erbB1 with filopodial actin filaments direct or indirect?

ErbB1 binds actin in vitro and the EGF high-affinity binding class of receptors are immunoprecipitated from cell extracts with antibodies to the actin cytoskeleton (den Hartigh et al., 1992), raising the possibility that the receptor binds directly to the actin bundle to initiate retrograde transport. However, in a more recent study, Stoorvogel et al. (2004) reported that mutation of the actin binding domain of erbB1 does not inhibit receptor uptake but rather abrogates downstream degradation. MCF7 cells were transfected with this mutant Δ989–994 erbB1 or wild-type erbB1, and EGF-QD binding and internalization were compared. Retrograde transport occurred equally in all transfected cells, demonstrating that erbB1 was not bound directly to F-actin filaments via this sequence motif.

Discussion

We have demonstrated at the single molecule level that a dimer of EGF-liganded and activated erbB1 receptors is the minimal species competent for transport along the filopodium toward the cell body (Fig. 5). The transport velocities of the erbB1-activated complex (Table I) were similar in all the cell types expressing either endogenous or transfected erbB1, independent of receptor expression on the cell surface, which ranged from 6×10^4 to 2×10^6 receptors/cell. Thus, the mechanism appears to be widespread and conserved. There was no significant difference in the transport rates over a temperature range of 23–37°C. Fewer loci were measured at the higher temperatures (Table I) due to the rapid movements of filopodia, making tracking of individual EGF-QD–erbB1 complexes difficult.

Although the actin cytoskeleton is required for transport, erbB1 does not bind directly to the actin filament through the reported actin-binding motif (amino acids 989–994 in the sequence). Our measured transport velocities on the filopodia fell within the range of values (up to 55 nm/s) reported for actin retrograde flow in vivo (Mallavarapu and Mitchison, 1999; Pollard and Borisy, 2003). In addition, we observed the same transport rate for EGF-QD–erbB1 and filopodial actin on Hela cells expressing an eGFP-actin. Although individual rates on different filopodia varied, the rates of multiple QD loci tracked on a given filopodium were the same. Values for actin poly-

merization are known to vary widely due to the action of auxiliary proteins, metabolite and energy sources, and cell type. The apparent correlation of the actin flow rate and erbB1 retrograde transport suggests that transport can occur without a motor protein such as myosin VI that transports in a retrograde direction toward the minus ends of actin filaments (Buss et al., 2004).

Diffusion constants in the range of $1–5 \times 10^{-10}$ cm^2/s were determined by FRAP and particle tracking measurements of liganded erbB1 on A431 cells, in which a large immobile fraction was also observed (Zidovetzki et al., 1981; Hillman and Schlessinger, 1982; Kusumi et al., 1993). We measured similar diffusion rates by FRAP for both the unliganded and liganded receptor using an erbB1-eGFP fusion protein stably expressed in A431 cells (Fig. 4). FCS measurements of erbB1-eGFP have yielded diffusion constants larger by an order of magnitude than those derived from FRAP (Brock et al., 1999b), probably due to the faster acquisition times and more restricted measurement volumes in FCS. The diffusion constants from EGF-QD tracking reported here are about half those determined by FRAP measurements. These differences may be due to the fact that our measurements of single molecules and small aggregates were acquired with a relatively long integration time and low acquisition frequency (200 ms at 1-s intervals), conditions that would obscure fast diffusion processes as shown by Murase et al. (2004). The size of the restricted diffusion area (0.15–0.3 μm^2) derived from the MSD plots was similar to that obtained by Kusumi et al. (1993) and implies that the receptor is organized in microdomains (Nagy et al., 2002) in variable states of association with the underlying cytoskeleton (Van Belzen et al., 1990; Yamabhai and Anderson, 2002). At the low temporal resolution of our measurements, the data may represent the rate of escape from such domains as well as intrinsic translational diffusion.

The discrete nature of the activation restricted to loci with bound ligand (Fig. 1) supports the thesis that the erbB1 receptor provides a very sensitive measure of the local ligand concentration. There have been reports of lateral signal propagation from activated erbB1 to unliganded molecules (Verveer et al., 2000). We have not observed such a phenomenon upon localized ligand presentation using EGF- or Herceptin-coupled magnetic microspheres to cells with receptor density varying between 6×10^4 and 2×10^6 (Fig. S3, available at http://

Figure 7. **Schematic depiction of filopodial retrograde transport of erbB1.** See text for details.

www.jcb.org/cgi/content/full/jcb.200503140/DC1; Brock and Jovin, 2001, 2003; Friedländer et al., 2005). Extensive propagation of activation between unliganded erbB1 molecules would also not result in the distinct diffusion and transport behavior documented in this study.

Our present view of directed transport along filopodia is depicted schematically in Fig. 7, indicating the conformational states and protein modifications of erbB1 that promote interaction with the F-actin filament and subsequent transport. The EGF receptor is present in either monomeric or oligomerized (not depicted) forms. Binding of EGF or EGF-QD (Fig. 7, green and red objects) leads to conformational rearrangements in ectodomain II (including extension of the dimerization loop; Garrett et al., 2002; Ogiso et al., 2002) and other domains (Fig. 7, black cytoplasmic region), potentiating the stabilization of an "active dimer" competent for auto- and transphosphorylation. The phosphoprotein (-P) interaction may be direct or mediated internally by adaptor proteins (Fig. 7, blue rectangles) leading to a physical linkage of the receptor complex to F-actin filaments (Fig. 7, black lines) and a shift from restricted diffusion (Fig. 7, pair of opposed arrows) to directed retrograde transport. The net velocity is given by the combination of the actin flow rate and motion of the adaptor link relative to the underlying actin filaments. Uptake into the cell body (not depicted) occurs at the base of the filopodium, where clathrin-coated pits and other components of the endocytic machinery are first available. As yet unresolved features of the retrograde transport mechanism are the identity of the adaptor proteins and/or receptor sequences, the locus and nature of cooperative interactions between activated receptors and the transport machinery, as well as loading and energetic considerations.

Biological roles of filopodial retrograde transport

This study indicates that a primary role for filopodia may be to serve as a sensory system for the cell by which they assist in regulating signal transduction pathways through transport of receptors once a given threshold of ligand binding is attained. It seems highly likely that filopodial retrograde transport is a general mechanism used by a wide range of cells, depending on the exact tissue and physiological context. Wound healing and embryonic development are obvious examples. Zieske et al. (2000) demonstrated in vivo in rat corneas that EGF, TGFα, heparin-binding EGF, and amphiregulin, which are all ligands of erbB1, are rapidly up-regulated in epithelial cells at the site of wounds. These cytokines stimulated erbB1 in neighboring cells and caused cell migration into the wound, whereas inhibition of the erbB1 kinase activity could be shown to inhibit migration. We have observed that vectorial application of EGF-QDs results in rapid formation of lamellipodia extending between the filopodia and cell movement in the direction of the gradient. Salas-Vidal and Lomeli (2004) proposed that filopodia and microvilli serve to regulate communication between the inner cell mass and the trophoectoderm in the mouse blastocyst. They demonstrated that growth factor and regulatory receptors, FGFR and erbB3, are distinctly and differentially enriched on these organelles dependent on the cell type. Other
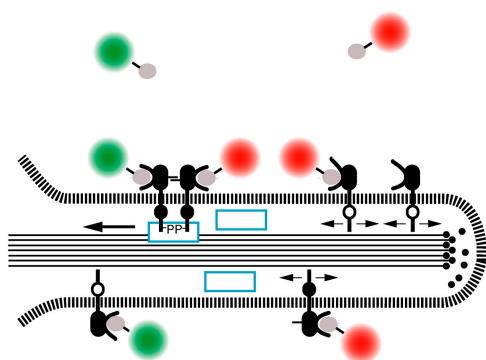
studies have documented the expression of all members of the erbB family as well as their ligands in the blastocyst in which orchestrated development requires that specific patterns of migration and differentiation be established and regulated (Paria and Dey, 1990; Wang et al., 2000).

Activation of tyrosine kinase membrane receptors requires dimerization mediated either through shared ligand binding or by ligand-induced increased affinity (as is the case for the erbB family; Yarden and Ullrich, 1988), and thereby provides a means for coupling ligand and receptor density to the regulation of downstream signaling. The discovery of retrograde transport of activated receptors on filopodia introduces a new, key feature in this regulatory mechanism.

Materials and methods

Reagents
All reagents were of analytical grade. Biotin-EGF, EGF, biocytin-Alexa594, and biocytin-Alexa546 were purchased from Molecular Probes. Qdot Streptavidin conjugates were obtained from Quantum Dot Corporation. PD153035, nocodazole, and cytochalasin D were purchased from Calbiochem. mAb CON.1 against clathrin light chain was purchased from Dianova. Antiphosphotyrosine 1068 (active erbB1) antibody was purchased from Cell Signaling Technologies. Live cell labeling was performed in Tyrode's buffer with 20 mM glucose and 0.1% BSA.

Plasmids and cell lines
ErbB1-eGFP expression plasmid was generated as described previously (Brock et al., 1999a) and erbB1 lacking six amino acids, the actin consensus binding sequence Δ989–994, was the kind gift of P. van Bergen en Henegouwen (Universiteit Utrecht, Utrecht, Netherlands). Transient transfections of HeLa, MCF7, or human adenocarcinoma A431 cells were performed with Lipofectamine 2000 (Invitrogen) or Effectene (QIAGEN). Some experiments were performed with stably transfected A431 or CHO cell lines expressing erbB1-eGFP. A commercial eGFP-actin plasmid (Invitrogen) was used to make a stably transfected HeLa cell line.

EGF and QD labeling of cells
EGF-QD ligand was formed by incubation of biotin-EGF (Molecular Probes) with 20 nM QDs at 4°C with mixing for >30 min in PBS. Most experiments were performed with a 6:1 or 3:1 molar ratio of biotin-EGF/QD. In the case of the low occupancy binding experiments, ratios of 3:1 or 1:1 were preformed and purified by size exclusion spin columns (P30; Bio-Rad Laboratories) to exclude free EGF molecules. Cells were grown in 8-well Lab-Tek chambers (Nunc) and imaged in Tyrode's buffer containing glucose and BSA. EGF-QD was added to cells at QD concentrations of 5 to 200 pM. For the two-color experiment, 90 nM EGF-QD525 and 30 nM EGF-QD605 were added simultaneously.

Cell treatments
Cells were typically starved (0.1% FCS) overnight. Cells were treated with inhibitors before measurement as follows: 15 μM nocodazole for 2 h at 37°C, 4 μM cytochalasin D for 30 min at 37°C, or 1 μM 153035 for 2 h at 37°C. Cells were maintained in the drugs during retrograde transport measurements.

Microscopy
Wide field detection of retrograde transport was recorded on a charge coupled device camera (model C4742-95; Hamamatsu) attached to a microscope (model Axiovert S100; Carl Zeiss MicroImaging, Inc.) with a 63× 1.4 NA oil immersion objective. Images were taken at 1-s intervals with 0.2-s integration times. QDs were excited at 436 nm with a bandpass filter and appropriate QD (20 nm) emission filters (Chroma Technology). Confocal laser scanning microscopy was performed with an LSM 510META (Carl Zeiss MicroImaging, Inc.) using a 63× 1.2 NA water or 63× 1.4 NA oil immersion objective with appropriate excitation and emission settings. Generally, three image planes at 0.5-μm steps were taken at 3-s intervals for all measurements. Deconvolution (as in Fig. 1) was performed using Huygens image processing software (Scientific Volume Imaging).

FRAP. Photobleaching data were acquired with an LSM 510META using a 63× 1.4 NA oil immersion objective. A431 cells expressing

erbB1-eGFP in the presence or absence of EGF-StreptavidinAlexa546 were imaged at low power (400–800 ms/image) with excitation at 488 and 532 nm. Photobleaching in a region of interest (2.2-μm-diam circle) was achieved by increasing the laser to full power. In the case where EGF-StreptavidinAlexa546 was added to the cells, the eGFP and Alexa546 were simultaneously imaged and bleached. Similarly, stably transfected HeLa cells expressing eGFP-actin were photobleached.

Two-color time series. QDs with different emission wavelengths were detected simultaneously using a microscope (model Axiovert S100) with the addition of an image splitter (either the Cairn Research Optosplit or a unit designed by R. Pick, Max Planck Institute for Biophysical Chemistry, Goettingen, Germany) containing appropriate QD (20 nm) bandpass emission filters in each channel in front of the ORCA-ER charge coupled device camera (Hamamatsu).

Data analysis
MSD calculations. QD loci were tracked over time using "View5D," an ImageJ (National Institutes of Health) plug-in developed by R. Heintzmann (King's College, London, England) that calculates the center of intensity in a region around the maximum at each time step, or similar routines written in Matlab (The MathWorks, Inc.). For diffusive behavior, the linear region of the MSD curves (first 10 points) was fit to either equation MSD = $2D\Delta t$ for PD153035-treated cells (the factor of two results from the one-dimensional geometry of the filopodia) or MSD = $4D\Delta t$ for cytochalasin-treated cells (the factor of four results from the two-dimensional geometry of wider filopodia induced by cytochalasin D), where D is the diffusion constant and Δt is the time interval (Kucik et al., 1989). D was calculated as the mean weighted by SD of the fit for each trace. The size of the restricted diffusion area was determined from the plateau in the MSD versus Δt plots. In the case of spots exhibiting a transition from the diffusion to the transport mode, only the active transport part of the trajectory was evaluated using the equation RMSD = $v\Delta t$, where v is the velocity of active transport (Kucik et al., 1989). This transition was found by visual inspection of the tracks in a time projection.

FRAP. Images were background subtracted and corrected for photobleaching during image acquisition. The post-bleach curves were fit to obtain the recovery half-time. The half-time and circular geometry of the bleach region were used to calculate the diffusion coefficient, D, as described in Axelrod et al. (1976).

Two-color tracking. The two different color channels acquired on the image splitter were registered using a calibration brightfield image taken at the beginning of the experiment. The QD loci were tracked separately for the different channels. The image processing was performed with DIPimage (Delft University of Technology).

Online supplemental material
Videos 1, 4, and 5 are QuickTime movies showing the retrograde transport of EGF-QD–erbB1 complexes as described in Figs. 2 A, 5 C, and 5 E, respectively. Videos 2 and 3 are QuickTime movies demonstrating the effects of Nocodazole and cytochalasin D, respectively, on retrograde transport. Fig. S1 shows the EGF-QDs are removed from the filopodia upon exposure to acid. Fig. S2 shows that clathrin is not present on the filopodia. Fig. S3 demonstrates the localized activation of erbB1 around EGF-labeled magnetic beads. Online supplemental material is available at http://www.jcb.org/cgi/content/full/jcb.200503140/DC1.

Note added in proof: After submission of this manuscript, a paper was published reporting an actin-dependent retrograde transport of NGF receptors on axonal growth cones (Tani, T., Y. Miyamoto, K.E. Fujimori, T. Taguchi, T. Yanagida, Y. Sako, and Y. Harada. 2005. *Neurosci.* 25:2181–2191).

References

Axelrod, D., D. Koppel, J. Schlessinger, E. Elson, and W. Webb. 1976. Mobility measurement by analysis of fluorescence photobleaching recovery kinetics. *Biophys. J.* 16:1055–1069.

Brock, R., and T.M. Jovin. 2001. Heterogeneity of signal transduction at the subcellular level: microsphere-based focal EGF receptor activation and stimulation of Shc translocation. *J. Cell Sci.* 114:2437–2447.

Brock, R., and T.M. Jovin. 2003. Quantitative image analysis of cellular protein translocation induced by magnetic microspheres: application to the EGF receptor. *Cytometry.* 52:1–11.

Brock, R., I.H.L. Hamelers, and T.M. Jovin. 1999a. Comparison of fixation protocols for adherent cultured cells applied to a GFP fusion protein of the epidermal growth factor receptor. *Cytometry.* 35:353–362.

Brock, R., G. Vamosi, G. Vereb, and T.M. Jovin. 1999b. Rapid characterization of green fluorescent protein fusion proteins on the molecular and cellular level by fluorescence correlation microscopy. *Proc. Natl. Acad. Sci. USA.* 96:10123–10128.

Buss, F., G. Spudich, and J. Kendrick-Jones. 2004. Myosin VI: cellular functions and motor properties. *Annu. Rev. Cell Dev. Biol.* 20:649–676.

Clapp, A., I. Medintz, J. Mauro, B. Fisher, M. Bawendi, and H. Mattoussi. 2004. Fluorescence resonance energy transfer between quantum dot donors and dye-labeled protein acceptors. *J. Am. Chem. Soc.* 126:301–310.

Dahan, M., S. Levi, C. Luccardini, P. Rostaing, B. Riveau, and A. Triller. 2003. Diffusion dynamics of glycine receptors revealed by single-quantum dot tracking. *Science.* 302:442–445.

den Hartigh, J.C., P.M. van Bergen en Henegouwen, A.J. Verkleij, and J. Boonstra. 1992. The EGF receptor is an actin-binding protein. *J. Cell Biol.* 119:349–355.

Friedländer, F., D.J. Arndt-Jovin, P. Nagy, T.M. Jovin, J. Szöllösi, and G. Vereb. 2005. Signal transduction of erbB receptors in trastuzumab (Herceptin) sensitive and resistant cell lines: local stimulation using magnetic microspheres as assessed by quantitative digital microscopy. *Cytometry.* In press.

Fry, D.W., A.J. Kraker, A. McMichael, L.A. Ambroso, J.M. Nelson, W.R. Leopold, R.W. Connors, and A.J. Bridges. 1994. A specific inhibitor of the epidermal growth factor receptor tyrosine kinase. *Science.* 265:1093–1095.

Garrett, T.P.J., N.M. McKern, M.Z. Lou, T.C. Elleman, T.E. Adams, G.O. Lovrecz, H.J. Zhu, F. Walker, M.J. Frenkel, P.A. Hoyne, et al. 2002. Crystal structure of a truncated epidermal growth factor receptor extracellular domain bound to transforming growth factor alpha. *Cell.* 110:763–773.

Goddette, D., and C. Frieden. 1986. Actin polymerization. The mechanism of action of cytochalasin D. *J. Biol. Chem.* 261:15974–15980.

Grecco, H.E., K.A. Lidke, R. Heintzmann, D.S. Lidke, C. Spagnuolo, O.E. Martinez, E.A. Jares-Erijman, and T.M. Jovin. 2004. Ensemble and single particle photophysical properties (two-photon excitation, anisotropy, FRET, lifetime, spectral conversion) of commercial quantum dots in solution and in live cells. *Microsc. Res. Tech.* 65:169–179.

Haigler, H.T., F.R. Maxfield, M.C. Willingham, and I. Pastan. 1980. Dansylcadaverine inhibits internalization of 125I-epidermal growth factor in BALB 3T3 cells. *J. Biol. Chem.* 255:1239–1241.

Hasson, T., and M.S. Mooseker. 1995. Molecular motors, membrane movements and physiology: emerging roles for myosins. *Curr. Opin. Cell Biol.* 7:587–594.

Helenius, A., J. Kartenbeck, K. Simons, and E. Fries. 1980. On the entry of Semliki forest virus into BHK-21 cells. *J. Cell Biol.* 84:404–420.

Hillman, G., and J. Schlessinger. 1982. The lateral diffusion of epidermal growth factor complexed to its surface receptors does not account for the thermal sensitivity of patch formation and endocytosis. *Biochemistry.* 21:1667–1672.

Jordan, M., D. Thrower, and L. Wilson. 1992. Effects of vinblastine, podophyllotoxin and nocodazole on mitotic spindles. Implications for the role of microtubule dynamics in mitosis. *J. Cell Sci.* 102:401–416.

Jorissen, R.N., F. Walker, N. Pouliot, T.P.J. Garrett, C.W. Ward, and A.W. Burgess. 2003. Epidermal growth factor receptor: mechanisms of activation and signalling. *Exp. Cell Res.* 284:31–53.

Kucik, D.F., E.L. Elson, and M.P. Sheetz. 1989. Forward transport of glycoproteins on leading lamellipodia in locomoting cells. *Nature.* 340:315–317.

Kusumi, A., Y. Sako, and M. Yamamoto. 1993. Confined lateral diffusion of membrane receptors as studied by single particle tracking (nanovid microscopy): effects of calcium-induced differentiation in cultured epithelial cells. *Biophys. J.* 65:2021–2040.

Lemmon, M.A., Z.M. Bu, J.E. Ladbury, M. Zhou, D. Pinchasi, I. Lax, D.M. Engelman, and J. Schlessinger. 1997. Two egf molecules contribute additively to stabilization of the egfr dimer. *EMBO J.* 16:281–294.

Lidke, D.S., P. Nagy, R. Heintzmann, D.J. Arndt-Jovin, J.N. Post, H.E. Grecco, E.A. Jares-Erijman, and T.M. Jovin. 2004. Quantum dot ligands provide new insights into erbB/HER receptor-mediated signal transduction. *Nat. Biotechnol.* 22:198–203.

Loomis, P.A., L.L. Zheng, G. Sekerkova, B. Changyaleket, E. Mugnaini, and J.R. Bartles. 2003. Espin cross-links cause the elongation of microvillus-type parallel actin bundles in vivo. *J. Cell Biol.* 163:1045–1055.

Mallavarapu, A., and T. Mitchison. 1999. Regulated actin cytoskeleton assembly at filopodium tips controls their extension and retraction. *J. Cell Biol.* 146:1097–1106.

Marmor, M.D., K.B. Skaria, and Y. Yarden. 2004. Signal transduction and oncogenesis by ErbB/HER receptors. *Int. J. Radiat. Oncol. Biol. Phys.* 58:903–913.

Mattoon, D., P. Klein, M.A. Lemmon, I. Lax, and J. Schlessinger. 2004. The tethered configuration of the EGF receptor extracellular domain exerts only a limited control of receptor function. *Proc. Natl. Acad. Sci. USA.* 101:923–928.

Murase, K., T. Fujiwara, Y. Umemura, K. Suzuki, R. Iino, H. Yamashita, M. Saito, H. Murakoshi, K. Ritchie, and A. Kusumi. 2004. Ultrafine membrane compartments for molecular diffusion as revealed by single molecule techniques. *Biophys. J.* 86:4075–4093.

Nagy, P., G. Vereb, Z. Sebestyén, G. Horváth, S.J. Lockett, S. Damjanovich, J.W. Park, T.M. Jovin, and J. Szöllösi. 2002. Lipid rafts and the local density or ErbB proteins influence the biological role of homo- and heteroassociations of ErbB2. *J. Cell Sci.* 115:4251–4262.

Ogiso, H., R. Ishitani, O. Nureki, S. Fukai, M. Yamanaka, J.H. Kim, K. Saito, A. Sakamoto, M. Inoue, M. Shirouzu, and S. Yokoyama. 2002. Crystal structure of the complex of human epidermal growth factor and receptor extracellular domains. *Cell.* 110:775–787.

Paria, B., and S. Dey. 1990. Preimplantation embryo development in vitro: cooperative interactions among embryos and role of growth factors. *Proc. Natl. Acad. Sci. USA.* 87:4756–4760.

Pollard, T., and G. Borisy. 2003. Cellular motility driven by assembly and disassembly of actin filaments. *Cell.* 112:453–465.

Salas-Vidal, E., and H. Lomeli. 2004. Imaging filopodia dynamics in the mouse blastocyte. *Dev. Biol.* 265:75–89.

Schlessinger, J. 2002. Ligand-induced, receptor-mediated dimerization and activation of EGF receptor. *Cell.* 110:669–672.

Small, J.V., T. Stradal, E. Vignal, and K. Rottner. 2002. The lamellipodium: where motility begins. *Trends Cell Biol.* 12:112–120.

Stoorvogel, W., S. Kersten, I. Fritzsche, J.C. den Hartigh, R. Oud, M. van der Heyden, J. Voortman, and P. van Bergen en Henegouwen. 2004. Sorting of ligand-activated epidermal growth factor receptor to lysosomes requires its actin-binding domain. *J. Biol. Chem.* 279:11562–11569.

Van Belzen, N., M. Spaargaren, A.J. Verkleij, and J. Boonstra. 1990. Interaction of epidermal growth factor receptors with the cytoskeleton is related to receptor clustering. *J. Cell. Physiol.* 145:365–375.

Verveer, P.J., F.S. Wouters, A.R. Reynolds, and P.I. Bastiaens. 2000. Quantitative imaging of lateral ErbB1 receptor signal propagation in the plasma membrane. *Science.* 290:1567–1570.

Wang, J., L. Mayernik, J. Schultz, and D. Armnat. 2000. Acceleration of trophoblast differentiation by heparin-binding EGF-like growth factor is dependent on the stage-specific activation of calcium influx by ErbB receptors in developing mouse blastocytsts. *Development.* 127:33–44.

Yambhai, M., and R.G.W. Anderson. 2002. Second cysteine-rich region of epidermal growth factor receptor contains targeting information for caveolae/rafts. *J. Biol. Chem.* 277:24843–24846.

Yarden, Y., and C. Ullrich. 1988. Growth factor receptor tyrosine kinases. *Annu. Rev. Biochem.* 57:443–478.

Yarden, Y., and M.X. Sliwkowski. 2001. Untangling the ErbB signalling network. *Nat. Rev. Mol. Cell Biol.* 2:127–137.

Zidovetzki, R., Y. Yarden, J. Schlessinger, and T.M. Jovin. 1981. Rotational diffusion of epidermal growth factor complexed to cell surface receptors reflects rapid microaggregation and endocytosis of occupied receptors. *Proc. Natl. Acad. Sci. USA.* 78:6981–6985.

Zieske, J.D., H. Takahashi, A.E.K. Hutcheon, and A.C. Dalbone. 2000. Activation of epidermal growth factor receptor during corneal epithelial migration. *Invest. Ophthalmol. Vis. Sci.* 41:1346–1355.